Cancer-cell Killing by Engineered *Salmonella* Imaged by Multiphoton Tomography in Live Mice

AISADA UCHUGONOVA[1-3], MING ZHAO[1], YONG ZHANG[1], MARTIN WEINIGEL[4], KARSTEN KÖNIG[3,4] and ROBERT M. HOFFMAN[1,2]

[1]*AntiCancer Inc., San Diego, CA, U.S.A.;*
[2]*Department of Surgery, University of California, San Diego, CA, U.S.A.;*
[3]*Department of Biophotonics and Laser Technology, Saarland University, Saarbrücken, Germany;*
[4]*JenLab GmbH, Jena, Germany*

Abstract. *Our laboratory has previously developed a bacterial cancer therapy strategy by targeting tumors using engineered Salmonella typhimurium auxotrophs (S. typhimurium A1-R) that were generated to grow in viable as well as necrotic areas of tumors but not in normal tissue. The mechanism by which A1-R kills cancer cells is unknown. In the present report, high-resolution multiphoton tomography was used to investigate the cellular basis of bacteria killing of cancer cells in live mice. Lewis lung cancer cells (LLC) were genetically labeled with red fluorescent protein (RFP) and injected subcutaneously in nude mice. After tumor growth was observed, the mice were treated with A1-R bacteria expressing GFP, via tail-vein injection. Mice without A1-R treatment served as untreated controls. The imaging system was 3D scan head mounted on a flexible mechano-optical articulated arm. A tunable 80 MHz titanium:sapphire femtosecond laser (710-920 nm) was used for the multiphoton tomography. We applied this high-resolution imaging tool to visualize A1-R bacteria targeting the Lewis lung cancer cells growing subcutaneously in nude mice. The tomographic images revealed that bacterially-infected cancer cells greatly expanded and burst and thereby lost viability. Similar results were seen in vitro using confocal microscopy. The bacteria targeted the tumor within minutes of tail-vein injection. Using mice in which the nestin-promoter drives GFP and in which blood vessels are labeled with GFP, the bacteria could be imaged in and out of the blood vessels. Collagen scaffolds within the tumor were imaged by second harmonic generation (SHG). The multiphoton tomographic system described here allows imaging of cancer cell killing by bacteria and can therefore be used to further understand its mechanism and optimization for clinical application.*

Correspondence to: Karsten König, e-mail: info@jenlab.de

Key Words: Tumor-targeting bacteria, *Salmonella typhimurium* A1-R, Lewis lung carcinoma, red fluorescent protein, RFP, DsRed, nude mice, multiphoton, tomography.

Bacteria have a long history of being able to elicit regression of tumors in human and animal models. In the late 19th and early 20th centuries, Coley developed bacterial therapy of cancer, first using bacteria, including *S. pyrogenes* and later extracts of the bacteria (Coley's toxins) to treat cancer patients. Although Coley did observe some antitumor efficacy in patients treated with toxins, live, replicating bacteria offer much more potential as cancer therapeutics (1-6).

Many types of bacteria have been shown to target tumors, but most are obligate anaerobes that grow only in the necrotic parts of tumors, thereby limiting their efficacy (7-9). Obligate anaerobes require combination with chemotherapy in order to regress tumors.

Salmonella, on the other hand, are facultative aerobes and can grow aerobically or anaerobically and, therefore, can grow in viable tumor tissue as well as necrotic tissue. Attenuated *Salmonella typhimurium* mutants, which grow in viable as well as necrotic areas of tumors, but not normal tissue, have shown particular effectiveness in mouse models of cancer (6).

A strain of *S. typhimurium* (VNP20009), attenuated by chromosomal deletion of the *purI* and *msbB* genes, was found to target tumors and inhibit tumor growth in mice. VNP20009 was tested on patients with metastatic melanoma and with metastatic renal cell carcinoma (10). Although the VNP20009 strain of *S. typhimurium* could be safely administered to patients, and tumor colonization was observed, no antitumor effect occurred. The lack of efficacy may be due to over-attenuation of VNP20009 (6).

We have developed a new substrain of *S. typhimurium*, A1-R, which has greatly increased antitumor efficacy, but due to auxotrophy for leu and arg, the strain can not mount a continuous infection in normal tissues. A1-R has no other

attenuating mutations. A1-R was able to effect cures in monotherapy in nude mouse models of metastatic human cancer (11).

A1-R was able to eradicate primary and metastatic tumors in monotherapy in nude mouse models of prostate, breast, and pancreatic cancer, as well as sarcoma and glioma (12-18). Tumors with a high degree of vascularity were more sensitive to A1-R as vascular destruction appears to play a role in A1-R antitumor efficacy (19).

We have also identified candidate *S. typhimurium* tumor-specific promoters that may enhance the antitumor efficacy of A1-R by driving expression of inserted therapeutic genes that could be selectively expressed in tumors (20, 21).

There has been intense interest to develop bacterial therapy of cancer using modern methods of bacterial genetics, cell and molecular biology, and *in vivo* imaging (6, 22). The barriers in tumors for standard therapy to be effective such as hypoxia, acidic pH, disorganized vascular architecture, and cancer-cell dissemination can be opportunities for bacteria to target cancer (22).

In addition, use of GFP for imaging the bacteria offers advantages of real-time visualization of single bacteria *in vivo* (23) which could lead to selection of enhanced cancer cell-targeting variants of *S. typhimurium*. For example, dual-color labeling of the cancer cells with GFP in the nucleus and red fluorescent protein (RFP) in the cytoplasm, allows simultaneous imaging of intracellularly-infecting GFP-expressing bacteria and apoptotic behavior of the infected cancer cells (12).

Multiphoton tomography based on two-photon excited fluorescence and second harmonic generation (SHG) is a powerful *in vivo* imaging technology. It provides optical sections with sub-micron resolution, high sensitivity (single-photon counting) and high penetration depth due to the use of infrared femtosecond laser pulses (24-26).

In order to further understand the mechanism of bacterial killing of cancer cells, the present report uses multiphoton tomography to visualize cancer cell killing by *S. typhimurium* A1-R in live mice.

Materials and Methods

Cancer cells. The Lewis lung carcinoma (LLC) cell line expressing GFP in the nucleus and RFP in the cytoplasm was used in *in vitro* experiments (27, 28). For *in vivo* experiments, the LLC cell line expressing RFP in the cytoplasm was used. For *RFP* gene transduction, 10% confluent LLC cells were incubated with a 1:1 precipitated mixture of retroviral supernatants of PT67 cells producing an *RFP* gene vector with a neomycin (G418)-resistant gene, and RPMI-1640 for 72 h. Fresh medium was replenished at this time. Lewis lung carcinoma cells were harvested by trypsin-EDTA 72 h post-transduction and subcultured at a ratio of 1:15 into selective medium that contained 200 μg/ml G418. The level of G418 was increased to 1000 μg/ml stepwise. The brightest Lewis Lung cells clones expressing RFP were selected, combined, and then amplified and transferred by conventional culture methods. In order to obtain dual-color cells, the histone H2B-GFP fusion gene was introduced to the Lewis lung carcinoma cells using similar methods as noted above (27, 28).

Mice. Twenty 6-week-old female nude mice, bred at AntiCancer Inc. (San Diego, CA, USA), were anesthetized with a 0.03 ml mixture of ketamine, acepromazine and xylazine Lewis lung carcinoma cells cells (2×10^6/100 μl Matrigel) were slowly injected s.c. into the flank of the nude mice (29). Additionally, nestin-GFP transgenic nude mice, with GFP expression driven by the nestin promoter [nestin-driven GFP (ND-GFP)] were used (30). All animal studies were conducted in accordance with the principals and procedures outlined in the NIH Guide for the Care and Use of Laboratory Animals under assurance of number A3873-1.

Preparation of S. typhimurium A1-R. GFP-expressing *Salmonella typhimurium* A1-R (AntiCancer Inc., San Diego, CA, USA) were grown overnight on Luria broth (LB) medium (Fisher Sci., Hanover Park, IL, USA) and then diluted 1:10 in LB medium. Bacteria were harvested at late-log phase, washed with phosphate buffered saline (PBS) and then diluted in PBS. Bacteria (5×10^7 CFU) were injected into the tail vein of mice, and then diluted in PBS (12-21, 23, 29-34).

Targeting Lewis lung carcinoma cells by S. typhimurium A1-R in vitro. LLC cells, labeled with GFP in the nucleus and RFP in the cytoplasm were grown on 6-well tissue culture plates in RPMI 1640 medium with 10% FBS to a density of 10^5 cells per well. *S. typhimurium* A1-R was grown in LB and harvested at late-log phase, diluted in cell culture medium and added to the cancer cells. After 45 min incubation at 37˚C, the cells were rinsed and cultured in medium containing gentamycin sulfate (20 μg/ml) to kill external but not internal bacteria. Interaction between bacteria and cancer cells was observed at different time points.

Multiphoton tomograph MPTflex. The multiphoton tomograph MPT*flex*™ (JenLab GmbH, Jena, Germany, and MultiPhoton Laser Technologies Inc., Irvine, CA) was equipped with a tunable 80 MHz titanium:sapphire femtosecond laser (710-920 nm). The optical unit consists of an active optical power attenuator to regulate the *in situ* power of the laser depending on tissue depth, an active beam stabilization device, a safety unit, and a flexible articulated mirror-arm with a compact scan head. The scan head consists of a fast galvo-scanning device to generate 2D (XY) scans, a piezodriven z-scanner, and high NA focusing optics (NA 1.3). The optical arm is stabilized with a mechanical arm. The scan head also contains a dual-photon detector unit for the measurement of autofluorescence and second harmonic generation (SHG). The overall field-of-view of the optical system covers 350×350 μm^2. The acquisition time for one optical section is typically 7 sec. Low picojoule pulse energy is used for multiphoton excitation. The PMT1924 photodetector was used to detect signals from both fluorescence and SHG channels. LP409 and BP395/14 filter sets were used for fluorescence and SHG, respectively (filter configuration I). To separate DsRed fluorescence from GFP- and autofluorescence, BP593/40 and BP510/42 filter sets were used, respectively (filter configuration II) (35, 36).

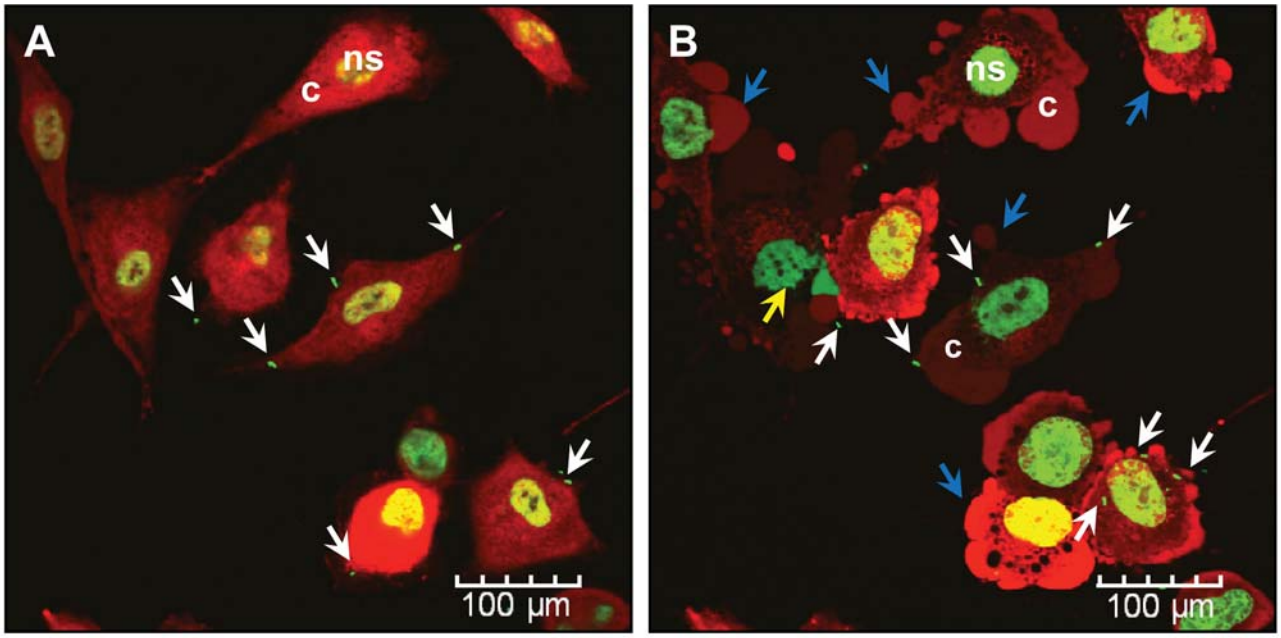

Figure 1. *In vitro imaging of dual-color LLC cancer cells expressing GFP in the nucleus (ns) and DsRed in the cytoplasm (c) during bacteria treatment. GFP-labeled double-auxotrophic mutant Salmonella typhimurium A1-R was applied to the LLC cancer cells. A: 10 min after treatment with bacteria. White arrows show bacteria invaded the cancer cells. B: The same cancer cells were monitored 45 min after treatment with S. typhimurium A1-R. The cancer cells expanded, burst, and lost viability. Blue arrows show microblebs. The yellow arrow shows a damaged nucleus. Cells were imaged with a confocal microscope at 473 nm for GFP excitation and 559 nm for DsRed excitation. Detection filters BA490-540 for GFP emission and BA575-675 for DsRed emission were used.*

Skin-flap windows. An arc-shaped incision (skin flap) was made in the skin, to image deeper into the tumor tissue. The skin flap could be opened repeatedly to directly image the cancer cells and simply closed with a 6-0 suture (37). The animals were anesthetized with a ketamine-mixture of Ketaset and PromAce (both from Fort Dodge Laboratories, Fort Dodge, IA, USA) and Xylazine HCl (American Animal Health, Wisner, NE, USA).

Confocal microscopy. Confocal microscopy (Fluoview FV1000, Olympus Corp., Tokyo, Japan) was used for imaging of dual-color LLC cells *in vitro* during bacteria treatment. Excitation wavelengths of 473 nm and 559 nm were used to excite GFP and DsRed respectively. Detection filters BA490-540 for GFP emission and BA575-675 for DsRed emission were used. Fluorescence images were obtained using the 40×/1.3 oil Olympus UPLAN FLN objective.

Results

In vitro experiments were performed on cell monolayers grown on 160-µm thick glass in special cell chambers. Dual-color LLC cancer cells expressing GFP in the nucleus and DsRed in the cytoplasm were monitored during *S. typhimurium* A1-R-GFP treatment (Figure 1). After *S. typhimurium* A1-R-GFP targeting, the LLC cells expanded, the membranes developed microblebs and the cells lost their characteristic morphology.

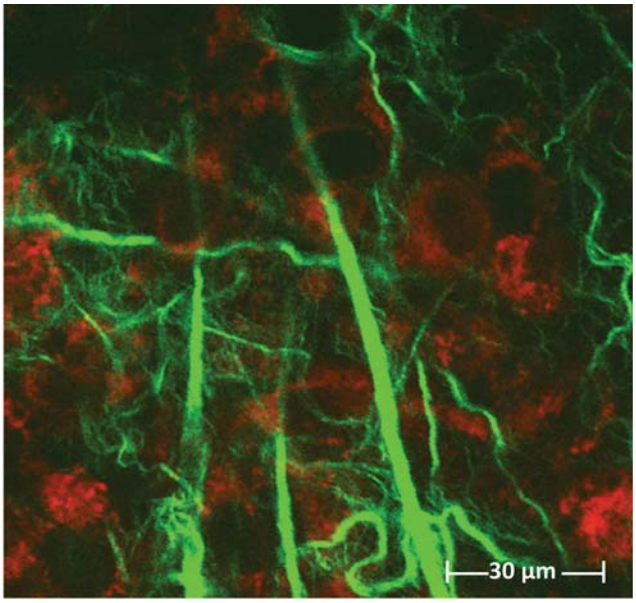

Figure 2. *Multiphoton fluorescence and SHG image of untreated LLC in live mice. Cancer cells express DsRed in the cytoplasm (red). The round nuclei appear dark. SHG from extracellular matrix collagen is depicted in green. DsRed was excited at 920 nm, and SHG at 790 nm (filter configuration I).*

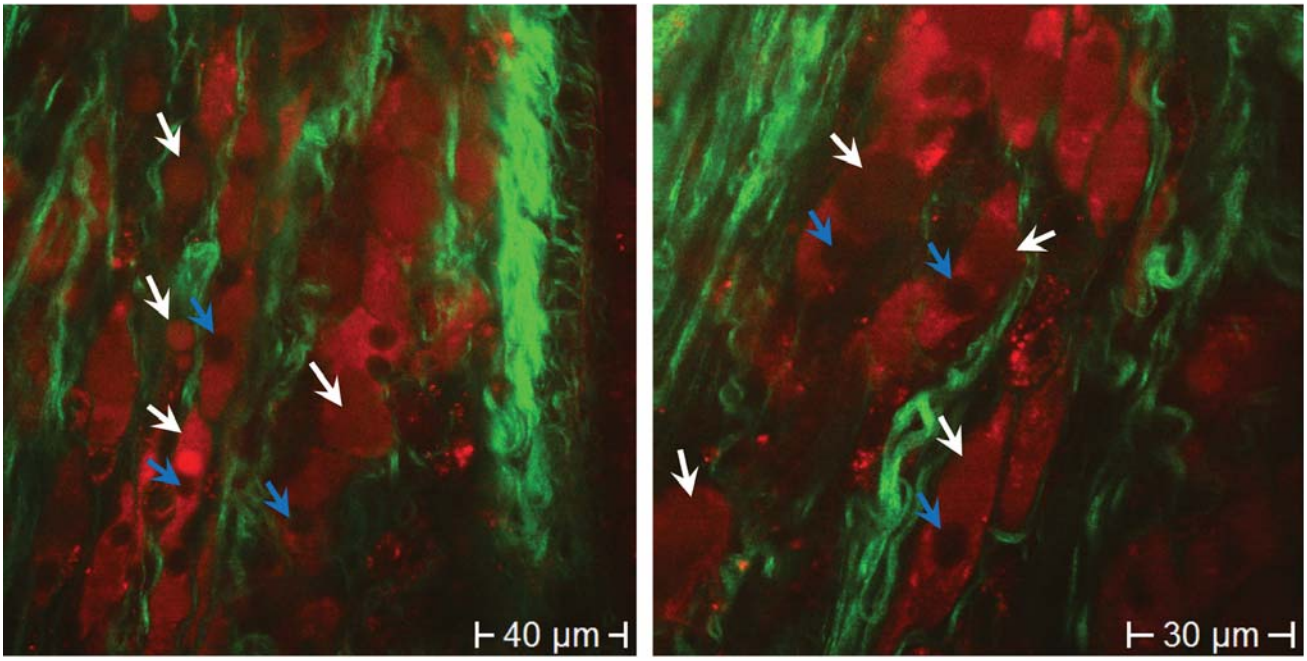

Figure 3. *Bacteria killing of cancer cells, observed by multiphoton tomography in live LLC tumor-bearing mice treated with A1-R bacteria. Extracellular matrix collagen was imaged by SHG without labeling (depicted in green color). Cancer cells expressing DsRed were visualized by two-photon excitation (red color). The tomographic images revealed that bacterially-infected cancer cells greatly expanded and burst and thereby lost viability similar to in vitro experiments (see Figure 1). DsRed was excited at 920 nm and SHG at 790 nm. Blue arrows show the cell nuclei. White arrows show microblebs and swollen cytoplasm.*

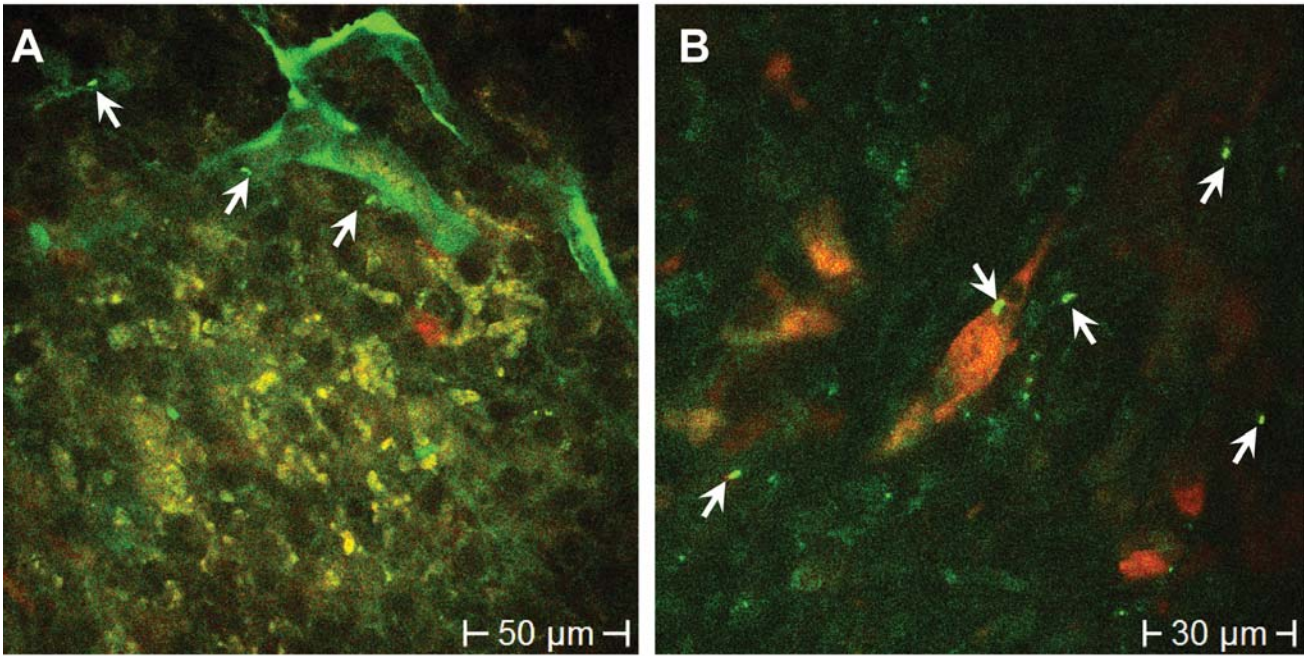

Figure 4. *In vivo multiphoton tomography with filter configuration II used to separate GFP, DsRed and autofluorescence signals. DsRed cancer cells (red), nestin-GFP-expressing capillaries, GFP-A1-R bacteria, and stromal cells (autofluorescence) were imaged in live mice. A: Mouse expressing nestin-GFP in capillaries was used to monitor bacteria invasion in the vessels. Single GFP-bacteria (white arrows) are seen inside and outside of capillaries. B: DsRed cancer cells, GFP-A1-R bacteria, and autofluorescent stromal cells were imaged by in vivo multiphoton tomography. White arrows demonstrate that GFP-expressing bacteria target the DsRed cancer cells several minutes after injection of bacteria into the tail vein.*

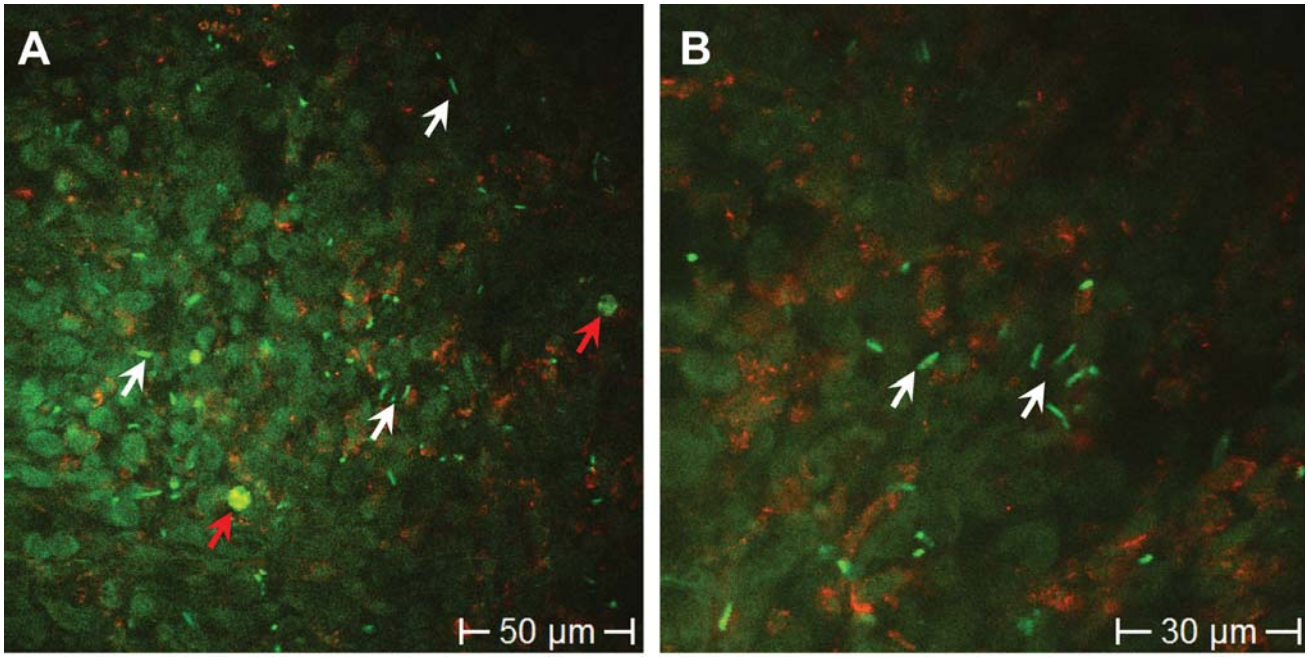

Figure 5. *In vivo imaging of an LLC tumor in a live mouse 2 days after treatment. Blue-green-yellow emission arises from autofluorescent stromal cells, red fluorescence from DsRed cancer cells, bright-green fluorescence from GFP-A1-R bacteria. Single bacteria (white arrows) and bacteria colonies (red arrows) are seen inside the tumor. Images A and B are taken with different magnification and from different areas of the tumor.*

Within hours, the nucleui of the cancer cells were destroyed and the cells burst and lost viability (Figure 1).

RFP (DsRed)-expressing cancer cells in living mice were monitored by multiphoton tomography (Figure 2). The extracellular matrix (ECM) collagen was monitored by SHG generation at 395 nm using a laser wavelength of 790 nm. The same laser wavelength (920 nm) was used to induce the fluorescence in the RFP-expressing cancer cells as well as in GFP expressing bacteria *via* two-photon excitation. Labeling of collagen was not required. DsRed was excited at 920 nm.

GFP-labeled bacteria (5×10^7) were injected into the tail vein. Two-photon imaging started some minutes later and was performed up to several hours. The tomographic images (Figure 3) revealed that bacterially-infected cancer cells greatly expanded and burst and thereby lost viability similar to what occurred *in vitro* (Figure 1). Microblebs were observed in the effected cancer cells.

In order to distinguish RFP-expressing cancer cells from GFP-expressing bacteria and autofluorescent stromal cells, the filter arrangement of the imaging system was modified. The broad band filter BP 593/40 was used to detect RFP in one detection channel. GFP and blue-green-yellow autofluorescence based on two-photon excitation of NADH (emission maximum 440-460 nm) and flavins/flavoproteins (emission maximum 530 nm) were detected using the BP510/42 filter in the second detection channel (filter configuration II) (Figure 4).

Nestin-GFP mice express GFP in nascent capillaries. Therefore it was possible to monitor bacteria inside vessels and their migration outside of the vessels into the tumor tissue (extravasation). Figure 4A shows single GFP bacteria inside and outside of capillaries. Cancer cells (red), A1-R bacteria (green), and stromal cells (autofluorescence) were detected simultaneously by multiphoton excitation. It was possible to monitor single GFP-expressing bacteria targeting RFP-expressing cancer cells in the tumor tissue several minutes after injection of bacteria into the tail vein (Figure 4B). RFP, GFP, and autofluorescence were recorded simultaneously with a single-laser scan and employment of two sensitive detectors based on single photon counting.

The effects of bacteria treatment are seen in Figure 5. Imaging of the tumor was performed on live mice 2 days after treatment. Blue-green-yellow emission arises from autofluorescence of stromal cells, red fluorescence from RFP-expressing cancer cells, and green fluorescence from GFP-bacteria A1-R. Single bacteria and bacteria colonies are seen inside the tumor. The cells looked unhealthy and necrotic.

Discussion

Multiphoton tomographs with flexible mechano-optical arms are optimal to perform 3D high-resolution nonlinear imaging of small animals. In the present report, we investigated cancer cell killing by engineered bacteria in tumor-bearing

living mice. We were able to image single intra-tissue bacteria, with a typical size of 1-5 μm, with *in vivo* multiphoton tomography with a lateral resolution between 300 nm and 500 nm. The *S. typhimurium* A1-R-GFP emitted green fluorescence, whereas the cancer cells fluoresced in the yellow spectral range due to cytoplasmatic RFP-expression (emission maximum: 583 nm). Furthermore, the non-labeled stromal cells were visualized by two-photon excited NAD(P)H autofluorescence. Extracellular non-labeled collagen was monitored by SHG.

Multiphoton tomography with it use of near infrared femtosecond laser radiation, therefore, provides a unique opportunity to image cancer cells in their native 3D microenvironement as well as tumor-targeting bacteria with subcellular resolution. Subcellular features such as nuclei as well as single intracellular bacteria can be imaged.

As shown in this study *S. typhimurium* bacteria are able to leave capillaries within minutes after i.v. injection and to start destruction of cancer cells within hours. The *in vivo* multiphoton tomographic system described here allows rapid imaging of cancer-cell killing by bacteria and can therefore be used to further understand its mechanism and optimization for clinical application.

Conflict of Interest

None of the authors have a conflict of interest in this study.

Acknowledgements

These studies were supported in part by National Cancer Institute grant CA126023.

References

1 Coley WB: Late results of the treatment of inoperable sarcoma by the mixed toxins of erysipelas and Bacillus prodigiosus. Am J Med Sci *131*: 375-430, 1906.
2 Coley WB: The treatment of malignant tumors by repeated inoculations of erysipelas: with a report of ten original cases. Am J Med Sci *105*: 487-511, 1893.
3 Coley-Nauths H, Fowler GA and Bogatko FH: A review of the influence of bacterial infection and bacterial products (Coley's toxins) on malignant tumours in man. Acta Med Scand *145*: 5-97, 1953.
4 Coley WB: Further observations upon the treatment of malignant tumors with the toxins of erysipelas and Bacillus prodigiosus with a report of 160 cases. Johns Hopkins Hosp Bull *7*: 175, 1896.
5 Thotathil Z and Jameson MB: Early experience with novel immunomodulators for cancer treatment. Expert Opin Investig Drugs *16*: 1391-1403, 2007.
6 Hoffman RM: The preclinical discovery of bacterial therapy for the treatment of metastatic cancer with unique advantages. Expert Opin Drug Discov *7*: 73-83, 2012.
7 Yazawa K, Fujimori M, Amano J, Kano Y and Taniguchi S: Bifidobacterium longum as a delivery system for cancer gene therapy: selective localization and growth in hypoxic tumors. Cancer Gene Ther *7*: 269-274, 2000.
8 Yazawa K, Fujimori M, Nakamura T, Sasaki T, Amano J, Kano Y and Taniguchi S: Bifidobacterium longum as a delivery system for gene therapy of chemically induced rat mammary tumors. Breast Cancer Res Treat *66*: 165-170, 2001.
9 Dang LH, Bettegowda C, Huso DL, Kinzler KW and Vogelstein B: Combination bacteriolytic therapy for the treatment of experimental tumors. Proc Natl Acad Sci USA *98*: 15155-15160, 2001.
10 Toso JF, Gill VJ, Hwu P, Marincola FM, Restifo NP, Schwartzentruber DJ, Sherry RM, Topalian SL, Yang JC, Stock F, Freezer LJ, Morton KE, Seipp C, Haworth L, Mavroukakis S, White D, MacDonald S, Mao J, Sznol M and Rosenberg SA: Phase I, study of the intravenous administration of attenuated *Salmonella typhimurium* to patients with metastatic melanoma. J Clin Oncol *20*: 142-152, 2002.
11 Hoffman RM: Bugging Tumors. Cancer Discovery *2*: 588-590, 2012.
12 Zhao M, Yang M, Li X-M, Jiang P, Baranov E, Li S, Xu M, Hoffman RM: Tumor-targeting bacterial therapy with amino acid auxotrophs of GFP-expressing *Salmonella typhimurium*. Proc Natl Acad Sci USA *102*: 755-760, 2005.
13 Zhao M, Yang M, Ma H, Li X, Tan X, Li S, Yang Z and Hoffman RM: Targeted therapy with a *Salmonella typhimurium* leucine-arginine auxotroph cures orthotopic human breast tumors in nude mice. Cancer Res *66*: 7647-7652, 2006.
14 Zhao M, Geller J, Ma H, Yang M, Penman S and Hoffman RM: Monotherapy with a tumor-targeting mutant of *Salmonella typhimurium* cures orthotopic metastatic mouse models of human prostate cancer. Proc Natl Acad Sci USA *104*: 10170-10174, 2007.
15 Nagakura C, Hayashi K, Zhao M, Yamauchi K, Yamamoto N, Tsuchiya H, Tomita K, Bouvet M and Hoffman RM: Efficacy of a genetically-modified *Salmonella typhimurium* in an orthotopic human pancreatic cancer in nude mice. Anticancer Res *29*: 1873-1878, 2009.
16 Hayashi K, Zhao M, Yamauchi K, Yamamoto N, Tsuchiya H, Tomita K, Kishimoto H, Bouvet M and Hoffman RM: Systemic targeting of primary bone tumor and lung metastasis of high-grade osteosarcoma in nude mice with a tumor-selective strain of *Salmonella typhimurium*. Cell Cycle *8*: 870-875, 2009.
17 Yam C, Zhao M, Hayashi K, Ma H, Kishimoto H, McElroy M, Bouvet M and Hoffman RM: Monotherapy with a tumor-targeting mutant of *S. typhimurium* inhibits liver metastasis in a mouse model of pancreatic cancer. J Surg Res *164*: 248-255, 2010.
18 Kimura H, Zhang L, Zhao M, Hayashi K, Tsuchiya H, Tomita K, Bouvet M, Wessels J and Hoffman RM: Targeted therapy of spinal cord glioma with a genetically-modified *Salmonella typhimurium*. Cell Prolif *43*: 41-48, 2010.
19 Liu F, Zhang L, Hoffman RM and Zhao M: Vessel destruction by tumor targeting *Salmonella typhimurium* A1-R is enhanced by high tumor vascularity. Cell Cycle *9*: 4518-4524, 2010.
20 Arrach N, Zhao M, Porwollik S, Hoffman RM and McClelland M: *Salmonella* promoters preferentially activated inside tumors. Cancer Res *68*: 4827-4832, 2008.
21 Arrach N, Cheng P, Zhao M, Santiviago CA, Hoffman RM and McClelland M: High-throughput screening for *Salmonella* avirulent mutants that retain targeting of solid tumors. Cancer Res *70*: 2165-2170, 2010.
22 Forbes NS: Engineering the perfect (bacterial) cancer therapy. Nat Rev Cancer *10*: 785-794, 2010.

23 Hoffman RM and Zhao M: Whole-body imaging of bacterial infection and antibiotic response. Nat Protoc *1*: 2988-2994, 2006.
24 König K and Riemann I: High-resolution multiphoton tomography of human skin with subcellular spatial resolution and picosecond time resolution. J Biomed Opt *8*: 432-439, 2003.
25 König K: Clinical multiphoton tomography. J Biophotonics *1*: 13-23, 2008.
26 König K, Raphael AP, Lin L, Grice JE, Soyer HP, Breunig HG, Roberts MS and Prow TW: Applications of multiphoton tomographs and femtosecond laser nanoprocessing microscopes in drug delivery research. Adv Drug Delivery Reviews *63*: 388-404, 2011.
27 Yamamoto N, Jiang P, Yang M, Xu M, Yamauchi K, Tsuchiya H, Tomita K, Wahl GM, Moossa AR and Hoffman RM: Cellular dynamics visualized in live cells *in vitro* and *in vivo* by differential dual-color nuclear-cytoplasmic fluorescent-protein expression. Cancer Res *64*: 4251-4256, 2004.
28 Hoffman RM and Yang M: Subcellular imaging in the live mouse. Nature Protoc *1*: 775-782, 2006.
29 Zhang Y, Tome Y, Suetsugu A, Zhang L, Zhang N, Hoffman RM and Zhao M: Determination of the optimal route of administration of *Salmonella typhimurium* A1-R to target breast cancer in nude mice. Anticancer Res *32*: 2501-2508, 2012.
30 Amoh Y, Yang M, Li L, Reynoso J, Bouvet M, Moossa AR, Katsuoka K and Hoffman RM: Nestin-linked green fluorescent protein transgenic nude mouse for imaging human tumor angiogenesis Cancer Res. *65*: 5352-5357, 2005.
31 Hayashi K, Zhao M, Yamauchi K, Yamamoto N, Tsuchiya H, Tomita K and Hoffman RM: Cancer metastasis directly eradicated by targeted therapy with a modified *Salmonella typhimurium*. J Cell Biochem *106*: 992-998, 2009.
32 Hoffman RM: Tumor-seeking *Salmonella* amino acid auxotrophs. Curr Opin Biotechnology *22*: 917-923, 2011.
33 Zhao M, Suetsugu A, Ma H, Zhang L, Liu F, Zhang Y, Tran B and Hoffman RM: Efficacy against lung metastasis with a tumor targeting mutant of *Salmonella typhimurium* in immunocompetent mice. Cell Cycle *11*: 187-193, 2012.
34 Momiyama M, Zhao M, Kimura H, Tran B, Chishima T, Bouvet M, Endo I and Hoffman RM: Inhibition and eradication of human glioma with tumor-targeting *Salmonella typhimurium* in an orthotopic nude-mouse model. Cell Cycle *11*: 628-632, 2012.
35 Uchugonova A, Hoffman RM, Weinigel M and König K: Watching stem cells in the skin of living mice noninvasively. Cell Cycle *10*: 2017-2020, 2011.
36 Uchugonova A, Duong J, Zhang N, König K and Hoffman RM: The bulge area is the origin of nestin-expressing pluripotent stem cells of the hair follicle. J Cell Biochem *112*: 2046-2050, 2011.
37 Yang M, Baranov E, Wang J-W, Jiang P, Wang X, Sun F-X, Bouvet M, Moossa AR, Penman S and Hoffman RM: Direct external imaging of nascent cancer, tumor progression, angiogenesis, and metastasis on internal organs in the fluorescent orthotopic model. Proc Natl Acad Sci USA *99*: 3824-3829, 2002.

Received August 29, 2012
Accepted September 12, 2012